

Electrical Properties of a One-dimensional Conductor, $\text{Na}_x\text{V}_2\text{O}_5$

Hayao KOBAYASHI

Department of Chemistry, Faculty of Science, Toho University, Chiba 274

(Received October 9, 1978)

The resistivity measurement, DTA analysis, refinement of the crystal structure, and examination of the X-ray diffuse scattering have been carried out on the β -phase of the sodium vanadium bronze. A resistivity minimum was observed around 200 K. The peak position of the logarithmic derivative of the resistance and an anomaly in the DTA curvature indicate that a metal-insulator transition occurs at about 130 K. The X-ray diffuse scattering shows a tendency of the sodium atoms toward cluster formation. It is concluded that the β -phase of sodium vanadium bronze is neither a simple one-dimensional metal nor a simple semiconductor, but can behave partly as a one-dimensional metal and partly as an anisotropic semiconductor.

Since the 1960's many investigations have been undertaken by solid state chemists in the field of vanadium oxide bronzes ($\text{M}_x\text{V}_2\text{O}_5$; $\text{M}=\text{Li}, \text{Na}, \text{K}, \text{Cu}, \dots$). It was at first commonly accepted that the materials lie near the critical donor concentration range required in the Mott theory for semiconductor-metal transitions and that the metal-metal spacing is approximately equal to the critical distance predicted by Goodenough for electron delocalization *via* d-orbital overlap.¹⁾ The early works seemed to establish that the charge transfer in vanadium bronzes is realized *via* the auto-localized electrons (polarons).^{2,3)} However, it has recently suggested that the β -phase vanadium bronzes should be considered as quasi-one-dimensional conductors.⁴⁾ Evidence for this view comes from (1) conductivity measurements which show that the anisotropy ($\sigma_{\parallel}/\sigma_{\perp}$) is 130 at room temperature ($\sigma_{\parallel}(\perp)$ is the conductivity parallel (perpendicular) to the *b* axis) and rises as high as 400 at 125 K;⁴⁾ (2) ESR measurements where the lineshape is asymmetric when the electric-field vector is parallel to the *b* axis, but Lorentzian for $E \perp b$,⁵⁾ and (3) optical reflectivity measurements which give a metallic plasma edge with light polarized along the *b* axis, but a featureless behaviour for perpendicular polarization.⁶⁾ In addition, recent investigation by Gunning *et al.*,⁷⁾ has shown that the dielectric constant is highly anisotropic and very large parallel to the *b* axis. This new view appears to conflict with the localization picture of the electron-conduction mechanism.

In this paper, we wish to present the results on our electrical conductivity, DTA measurements, structure refinement, and examination of the X-ray diffuse scatterings of the β -phase of the sodium vanadium bronze (β -NaVB).

Experimental

Preparation of Samples. The samples of the sodium vanadium bronze were prepared in a quartz boat. A 6 : 1 mixture of V_2O_5 and Na_2CO_3 or a 1 : 1 mixture of NaVO_3 and V_2O_5 was heated for 17 h at 700 °C in an air atmosphere and then cooled at a rate of 6 °C/h.^{1,8)} The black needle-shaped crystals were pried out of the quartz boat. Examination by X-ray diffraction revealed that the crystals are monoclinic with the Wadsley β -type structure.⁸⁾

Refinement and Brief Description of the Crystal Structure. The crystal structure of β -NaVB was determined in the

1950's by Wadsley⁸⁾ and by Ozerov *et al.*⁹⁾ Considering the fundamental significance of the Wadsley β -structure²⁾ and the relatively large *R* index (the *R* indices for *h*0*l* and 0*kl* are 0.17 and 0.13 respectively⁸⁾), the crystal structure refinement would be desirable. Since our measurements were made before the publication of the works of Wallis *et al.*⁴⁾ and [Kaplan and Zylbersztein,⁶⁾ which have first suggested a "one-dimensional metallic character" of this compound, our observation seemed to be inconsistent with the semiconducting behavior previously accepted. At first sight, this discrepancy appears to be attributable to a slight change in the crystalline state, one which might be introduced in the stage of the sample preparation, because our samples were prepared in quartz boats, whereas the other authors used platinum boats or platinum dishes. The purpose of the structure refinement was partly to examine this possibility.

The lattice constants were determined using a computer-controlled four-circle diffractometer. The crystal data are: monoclinic, space group C2/m ,¹⁰⁾ $a=16.435(16)$ Å, $b=3.612(1)$, $c=10.086(10)$, $\beta=109.61(15)^\circ$, $D_x=3.55$ gcm⁻³, $Z=6$ ($\text{Na}_x\text{V}_2\text{O}_5$; $x=0.287$ (see Appendix)).

Some details of the structure refinements, the atomic coordinates, and the bond lengths and angles around the vanadium atoms are given in Appendix. There is no serious difference between the newly refined structure and the previously determined one.

The crystal structure is shown in Fig. 1. The unit cell contains three crystallographically independent vanadium sites. As was pointed out by Wadsley,⁸⁾ the coordination of vanadium is of two kinds. V(1) and V(2) are each linked to six oxygens disposed at the corners of strongly distorted octahedra. The octahedra are associated in pairs, with a shared edge which unites with similar pairs above and below to form a zigzag ribbon extending along the *b* axis (Fig. 2a). On the other hand, V(3) has five bonds to oxygen to form trigonal bipyramids, which are associated in pairs to form a double chain by each having an edge in common with each V(3) neighbour (Fig. 2b). The short distance between the vanadium ions (Figs. 1 and 2) appears to allow the formation of delocalized states arranged in linear chains along the *b* axis.⁵⁾ The sodium atoms lie at random in two rows in the tunnels formed by the vanadium and oxygen atoms as a whole (Fig. 3). The distance between two sodium sites is only 1.95 Å. With an increase in the sodium content ($\text{Na}_x\text{V}_2\text{O}_5$; $0.2 < x < 0.33$), the sodium sites are gradually filled; the occupancy probability is 50% if $x=1/3$. Because of the Coulomb interaction, sodium ions will tend to be arrayed regularly. In fact, a tendency for the regular arrangement of sodium atoms has been revealed by the examination of oscillation photographs, which will be described later.

Resistivity Measurements. The d.c. electrical resistivities were measured over the temperature range of 78 K—

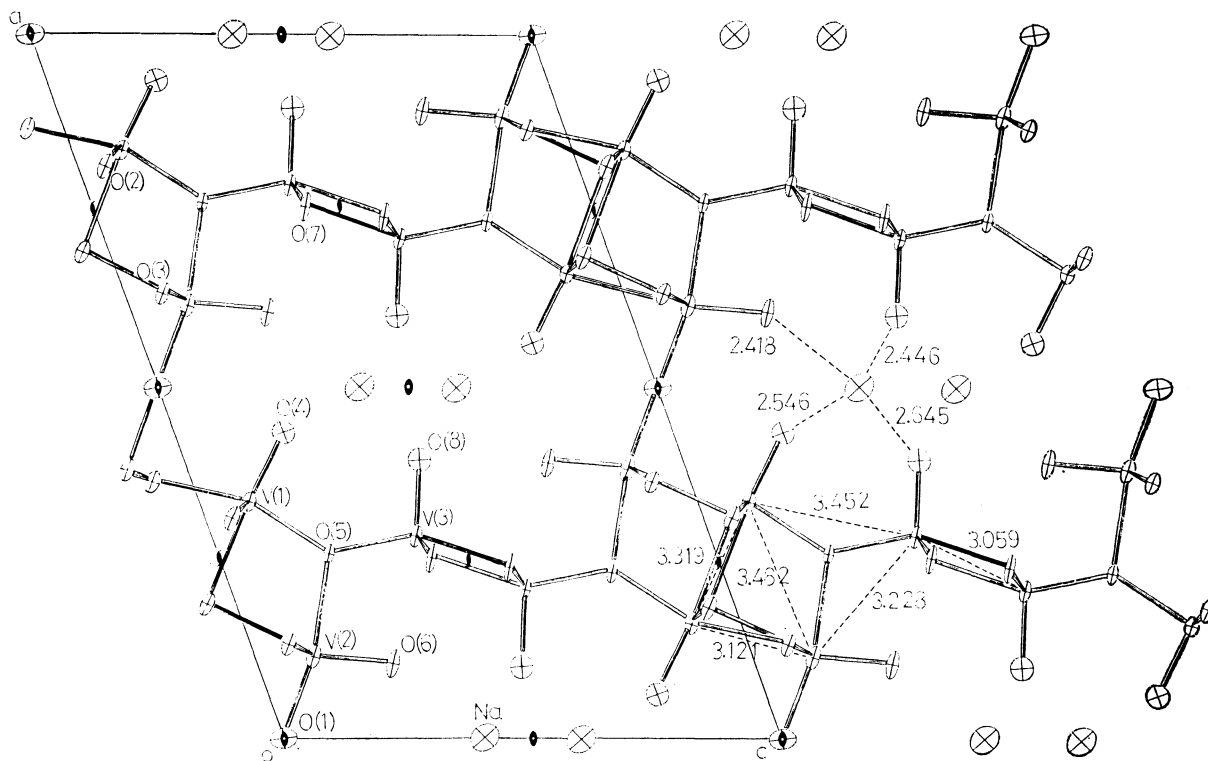


Fig. 1. Projection of the crystal structure.

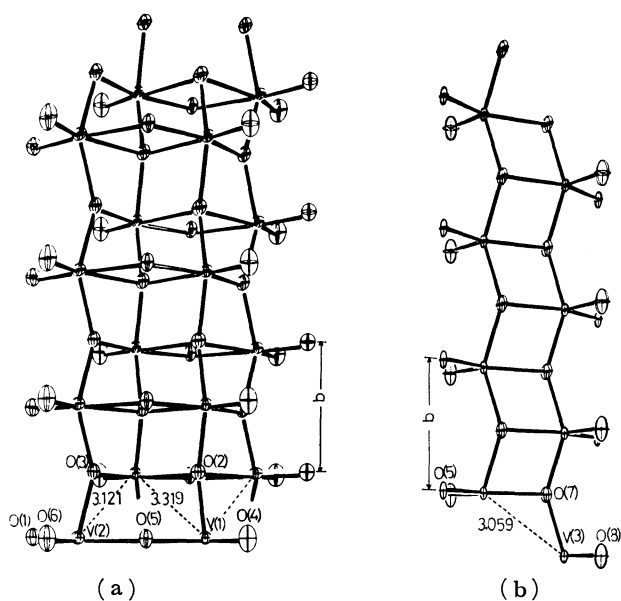


Fig. 2. Perspective view of the "chain structures" of the vanadium and oxygen atoms.

(a) A complex chain constructed of the 6-coordinated vanadium atoms (V(1) and V(2)). (b) A double chain of the 5-coordinated vanadium atoms (V(3)).

600 K for several specimens along the needle axis (the *b* axis) of the crystals using a four-probe method. The crystals were washed with aqueous NH_3 . Gold wires 0.025 mm in diameter were bonded to the crystals by silver conducting paint (Shoei 4895). Then the crystals were annealed for about 30 min at about 300 °C. The sample dimensions and probe separations were measured with a microscope. Because of the uncertainty in determining the exact probe separation and sample dimensions, the estimated error in

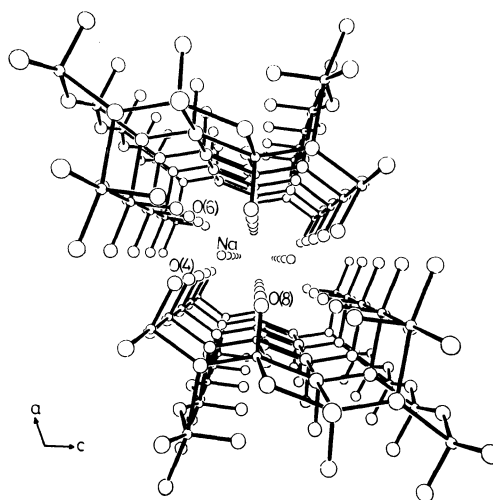


Fig. 3. Perspective view of the tunnel structure.

the resistivities is about 50%. The results are shown in Figs. 4 and 5. The room-temperature resistivity is $6.0 \pm 3.0 \times 10^{-8} \Omega \text{ cm}$. The logarithmic derivative of the resistance, $-(d \ln R/dT)$, versus the temperature is also shown in Fig. 4. In a one-dimensional conductor, a metal-insulator (M-I) transition temperature is defined by the peak position of $-(d \ln R/dT)$ versus T .^{11,12} The inset of Fig. 4 shows a peak around 130 K.

DTA Experiments. A quasi-one-dimensional conductor exhibits a specific heat anomaly in the temperature range around the M-I transition temperature.^{13,14} Judging from the anisotropy of the electric conductivity and the optical reflectivity, the peak of the $d \ln R/dT$ vs. T curvature around 130 K (Fig. 4) can be considered to be an indication of the occurrence of a M-I transition. The DTA measurements were made to obtain further evidence.

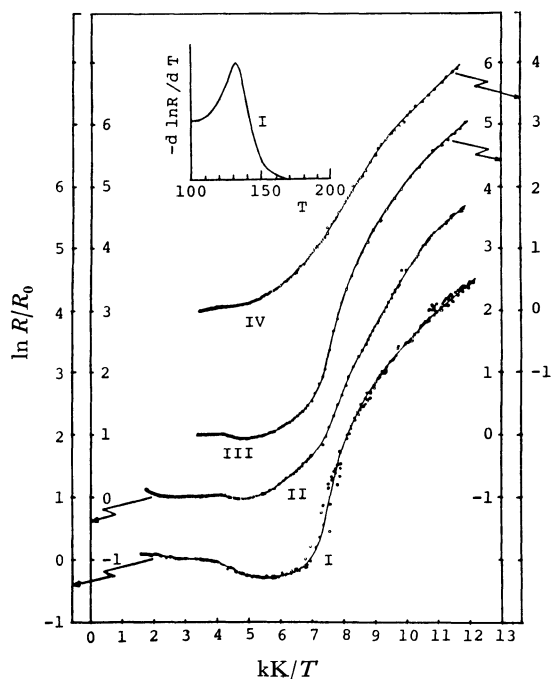


Fig. 4. Logarithm of normalized resistivity *versus* inverse temperature. The inset shows $-(d \ln R / dT)$ *versus* T . Curvatures I—IV indicate the resistivities of four different samples.

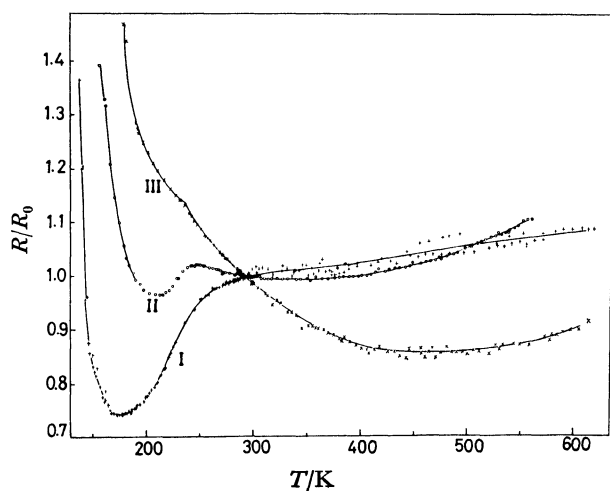


Fig. 5. The temperature dependence of the normalized resistivity. Curvatures I, II, and III show the resistivities of the samples I, II, and IV in Fig. 4, respectively.

The crystals of β -NaVB were ground in a glass mortar and mixed thoroughly with an approximate amount of powdered almina. A copper-Constantan thermocouple was embedded in a quantity of the mixed powder placed in a hole ($50 \text{ mm} \times 6 \text{ mm}$) in a cylindrical copper block. The reference thermocouple and the thermocouple used for temperature measurements were in the other two holes, packed with powdered almina. The DTA measurements were made by warming or cooling the copper block. The rate of temperature change was controlled by raising or lowering a liquid-nitrogen vessel with respect to the copper block. Since a small anomaly was observed in the first run, the measurements were repeated eight times to confirm it. On the repeated runs, however,

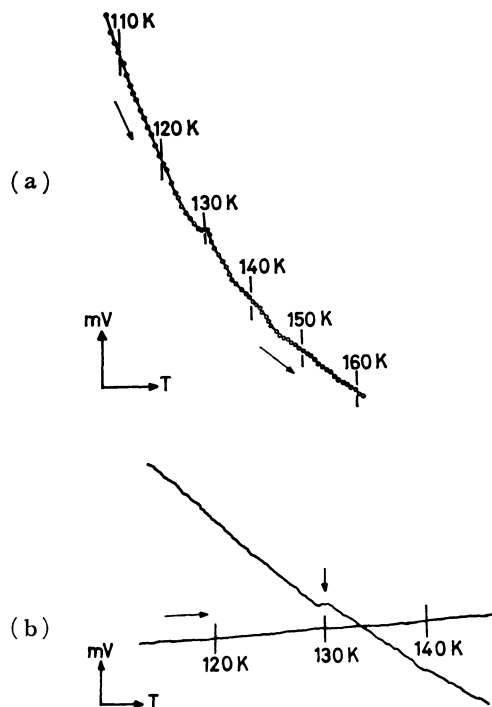


Fig. 6. (a) Averaged thermogram obtained from eight warming curves. (b) An example of the warming curves.

only the warming cycles were examined because of the facility of the temperature control. The voltage readings of the eight thermograms were then added. The dependence on the temperature is shown in Fig. 6a. An anomaly was observed at about 130 K. The measurements were repeated on another sample in order to confirm the reproducibility of the anomaly (Fig. 6b). The heat of transition was roughly estimated to be 10–20 cal/mol by reference to the thermograms of NH_4Cl ($T_c = 242.8 \text{ K}$, 0.20 kcal/mol) and $\text{NH}_4\text{H}_2\text{PO}_4$ ($T_c = 148 \text{ K}$, 0.15 kcal/mol).

X-Ray Diffuse Scatterings. X-Ray diffuse scatterings associated with the one-dimensional charge-density waves are among the most direct indications of the metallic state of a system. Besides this, another type of X-ray diffuse scattering can also be expected in β -NaVB. Although crystal-structure analysis shows that the sodium atoms are randomly distributed in two rows in the tunnels, a short-range order among the sodium atoms, which gives rise to X-ray diffuse scatterings, also exists.

Oscillation photographs around the b axis were taken at room temperature using Ni-filtered $\text{Cu K}\alpha$ radiation. The exposure times were about 100 h. An example of the photographs is shown in Fig. 7. Weak and broad scatterings are observed between strong layer lines. The existence of the diffuse scatterings was confirmed by comparing the photograph with one taken without mounting a crystal on a glass capillary.

The X-ray diffuse scattering associated with a one-dimensional distortion or a Kohn anomaly generally consists of diffuse, narrow streaks¹⁵⁾ and is inconsistent with the breadth of the observed diffuse scattering. The diffuse scatterings in the middle of the sharp layer lines indicates a tendency of the doubling of the lattice spacing along the b axis. Wadsley has suggested that sodium atoms in a tunnel alternately occupy one of the two possible sites to form a staggered string.⁸⁾ If this suggestion were true, the lattice spacing would be doubled along the b axis. Actually, the mode of

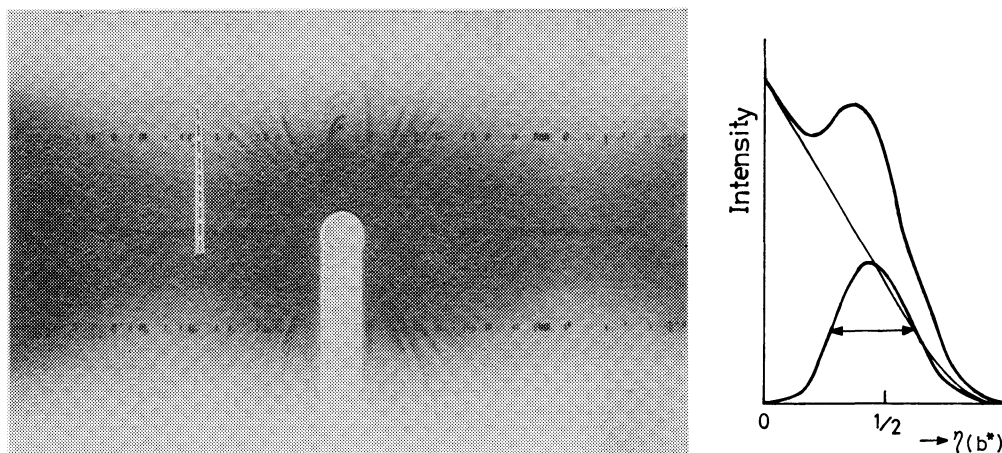


Fig. 7. Oscillation photograph around the b axis and the scattering intensity along the dashed line.

the arrangement of sodium atoms is even more complicated because of the nonstoichiometry of the sodium content. The staggered strings may be interrupted. Consequently, the diffuse scatterings may be attributable to existence of "imperfect staggered strings." The constant scattering intensity along the direction perpendicular to b implies that the correlation between sodium atoms belonging to different tunnels is weak. If the "correlation length ξ " can be estimated by $\xi \approx 2/\Gamma^{16)}$ (Γ is the full width at a half maximum of the diffuse scatterings), it is of the order of 20 Å for the b direction (the width of the "diffuse belt" is about $0.35 b^*$).

Discussion

The room-temperature conductivity of 200 ± 100 ($\Omega \text{ cm}$) $^{-1}$ agrees with those values reported by Sienko and Sohn (230 ($\Omega \text{ cm}$) $^{-1}$) $^{17)}$ and Wallis, Sol, and Zylbersztejn (110 ($\Omega \text{ cm}$) $^{-1}$) $^{4)}$; it is also of the same order as that of the well-known one-dimensional metal $\text{K}_2\text{Pt}(\text{CN})_4\text{Br}_{0.3} \cdot 3\text{H}_2\text{O}$ (≈ 500 ($\Omega \text{ cm}$) $^{-1}$) $^{18)}$. In addition, it is compatible with the optical conductivity along the b axis (250 ($\Omega \text{ cm}$) $^{-1}$) as calculated from $\sigma_{\text{opt}} = \omega_p^2 \tau / 4\pi$ using the plasma frequency ($\omega_p = 1.44 \times 10^{15} \text{ s}^{-1}$) and the electronic relaxation time ($\tau = 1.35 \times 10^{-15} \text{ s}$) reported by Kaplan and Zylbersztejn. $^{6)}$ Needless to say, this agreement does not necessarily support a "simplified one-dimensional metal picture" of this compound. Some crystals show small, but distinct, resistivity minima around 200 K, and the other crystals give an indication of resistivity minima by means of their concave curvatures (Figs. 4 and 5). This is the first observation of the resistivity minimum. However, similar resistivity-*vs.*-temperature behaviour can also be found in papers previously reported: (1) $\log \sigma$ plotted against $1/T$ of Wallis *et al.* $^{4)}$ shows a distinct concave curve upwards around 180 K, implying a latent conductivity maximum. (2) Despite the small number of the datum points, a deviation from the smooth curve of resistivity *versus* the inverse temperature around 200 K can be found reported in the paper of Sienko and Sohn. $^{17)}$

The existence of the relatively sharp minimum (Fig. 5) shows the non-semiconductive character of the compound. When the resistivity minimum is sharp, the logarithmic derivative of the resistance *versus* temperature gives a well-defined peak at about

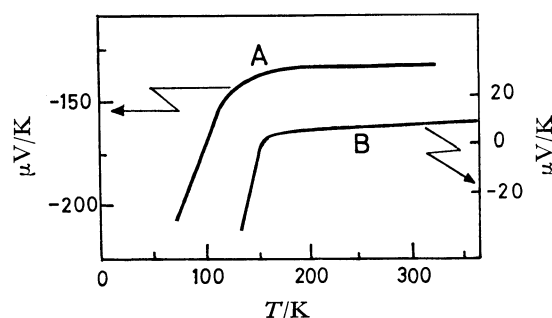


Fig. 8. Seebeck coefficient *versus* temperature of β -NaVB (A) (Ref. 1) and that of one-dimensional conductor, $(\text{TTF})_{12}(\text{SCN})_7$ around its M-I transition temperature ($T_c = 169 \text{ K}$) (B) (Ref. 12).

130 K, which suggests that the phase transition observed by DTA measurements is a M-I transition. The ratio of the low-temperature activation energy to the M-I transition temperature, Δ/T_c , is approximately constant in one-dimensional systems ($\Delta/T_c = 5 \pm 1$). Wallis *et al.* $^{4)}$ reported that the conductivity shows a simple activated behaviour between 80 K and 125 K, the activation energy being 61 meV ($= 708 \text{ K}$). The Δ/T_c ratio is 5.5. Some observations indicating a phase transition can also be seen in the literature: (1) The Seebeck coefficient is almost constant when $T > 150 \text{ K}$ and decreases abruptly when $T < 110 \text{ K}$; that is, the temperature dependence changes around T_c ($\approx 130 \text{ K}$) (Fig. 8). $^{1)}$ (2) The susceptibility follows a Curie-Weiss law from 150 K to 450 K, but its temperature dependence becomes more complicated when $T < T_c$. $^{19)}$ (3) The anisotropy of the conductivity reaches a maximum ($\sigma_{\parallel}/\sigma_{\perp} \approx 400$) at 125 K ($\approx T_c$).

Thus, the occurrence of the M-I transition appears to be confirmed. On the other hand, on the basis of an examination of the temperature dependence and the anisotropy of electric conductivity, Wallis *et al.* have shown that a variable-range hopping model is applicable at low temperatures ($T < 80 \text{ K}$) and have proposed an interrupted strand model. $^{4)}$ ESR study by Friederich *et al.* has suggested that the sodium ions are clustered rather than being distributed randomly among

possible sites in the tunnel structure, and that a crystal is separated into regions where the electron concentration is fixed at the value corresponding to $x=1/3$.¹⁹⁾ This picture provides a basis for the interrupted strand model of the electronic-transport mechanism. As has been described above, the observation of diffuse X-ray scattering gives more direct evidence for the "cluster formation" of sodium atoms.

Thus, β -NaVB can be regarded as neither a simple metal nor a simple semiconductor; rather, it has the following two aspects: (1) a one-dimensional metallic character originating from the delocalization states arranged in a linear chain along the b axis,⁵⁾ and (2) a semiconductive nature due to the localization of the electron.

On the basis of this information, the temperature variation in Seebeck coefficient will now be interpreted. The room-temperature Seebeck coefficient of $\text{M}_x\text{V}_2\text{O}_5$ ($\text{M}=\text{Na}, \text{Cu}, \text{Ag}; 0.2 < x < 0.6$) has been explained by Goodenough in terms of a small polaron formula.²⁾ Since a Seebeck coefficient, α , is generally small in a metallic state, the large room-temperature value of $135 \mu\text{V/K}$ (Fig. 8)¹⁾ appears to be inconsistent with the observation of metallic behaviour around room temperature. However, if α includes the sum of α_A (the contribution from the "metallic part"), and α_B (the contribution from the "semiconductive part"), the large room-temperature value can be attributed to α_B . When a one-dimensional metal undergoes a M-I transition, the magnitude of the Seebeck coefficient (α_A) increases abruptly (Fig. 8).^{12,20)} Thus, the temperature variation of α can be explained.

Figure 9 shows a typical example of the resistivity behaviour of a one-dimensional metal around the M-I transition temperature (A) and that of a variable-range hopping mechanism in a disordered semiconducting system (B).^{4,21)} The sample dependence of the resistivity (Fig. 5) can be interpreted by the superposition of A and B, if the contribution of A (R_A) and B (R_B) to the resistivity vary from sample to sample ($R=R_A+R_B$). Below the M-I transition temperature, R_A increases exponentially with a decrease in the temperature. Therefore, the magnitude of the resistivity can be mainly determined by the variable-range hopping process ($R \approx R_B$). In fact, Wallis *et al.* have pointed out that the activation energy decreases smoothly below 80 K. On the other hand, at high temperatures R is approximately equal

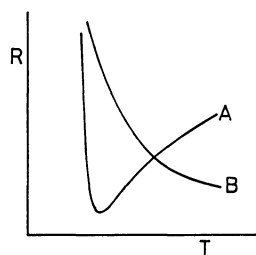


Fig. 9. Schematic illustration of the resistivity *versus* temperature curve of a one-dimensional metal around the M-I transition temperature (A) and that by one-dimensional variable range hopping conduction (B).

to R_A and the "metallic conductivity" may be observed.

It is well-known that small amounts of disorder and defects in a crystal have a great influence on the electrical conductivity and frequently smear out the M-I transition.^{12,22)} Kapuskin *et al.* have reported that the lattice parameters of $\text{M}_x\text{V}_2\text{O}_5$ ($\text{M}=\text{Li}, \text{Na}, \text{K}$) are changed slightly by the evolution of oxygen on heating to 730–780 K.²³⁾ Although no more than 0.7 atoms of oxygen are evolved from one elementary cell of bronze, a drastic change in electronic properties is produced. As has been mentioned before, the crystals of β -NaVB were prepared at about 700 °C and then cooled at a rate of 6 °C/h. Since the reaction temperature is higher than 730–780 K, it may be possible that a slight modification is made in the crystalline state, which then gives rise to a sample dependence of the electrical resistivity.

In conclusion, β -NaVB appears to be a non-stoichiometric compound which can behave partly as a one-dimensional metal and partly as an anisotropic semiconductor. The chain-like structure of vanadium and oxygen atoms and a tendency towards the formation of disordered strings of sodium atoms accommodated in the tunnels provide a structural background for this picture of the compound.

Appendix

Refinement of the Crystal Structure. The intensity data were collected with a Rigaku automated four-circle diffractometer using $\text{Mo K}\alpha$ radiation. There are 1180 independent reflections ($|F_o| > 3\sigma(|F_o|)$) up to $2\theta \leq 70^\circ$. The systematic absences indicate the space group to be C2/m , Cm , or C2 . The $N(z)$ test and the statistical intensity distribution of $|E|(hkl)$ favoured the centrosymmetrical group; the space group was, therefore, assumed to be C2/m .¹⁰⁾ The atomic parameters and the occupancy probability of the sodium site were refined by a full-matrix least-squares method. The final R -factor is 0.038. The occupancy probability becomes 43% ($\text{Na}_x\text{V}_2\text{O}_5$; $x=0.287$) for the crystal subjected to this structure refinement. The positional and thermal parameters are given in Table 1. The structure

TABLE 1. ATOMIC COORDINATES ($\times 10^5$)
Their standard deviations are in parentheses.

	x	y	z
V(1)	33757(7)	0	10079(10)
V(2)	11624(8)	0	11885(11)
V(3)	28791(7)	0	40997(10)
Na ^{a)}	99(54)	0	40367(84)
O(1)	0	0	0
O(2)	81425(33)	0	5535(49)
O(3)	63373(32)	0	7802(47)
O(4)	43625(35)	0	21898(54)
O(5)	26323(31)	0	22299(45)
O(6)	10674(37)	0	27294(51)
O(7)	75701(36)	0	42520(48)
O(8)	39762(36)	0	47111(54)

a) The occupation probability is 43%.

TABLE 2 INTERATOMIC DISTANCES
 Bond lengths and angles around vanadium atoms.

Symmetry code					
None	x, y, z	i	$1-x, y, -z$		
ii	$-1/2+x, 1/2+y, z$	iii	$1-x, y, 1-z$		
iv	$1/2-x, 1/2+y, 1-z$	v	$-x, y, 1-z$		
V(1)...O(4)	1.588(5) Å	V(1)...O(5)	1.945(5)		
V(1)...O(2) _i	2.344(4)	V(1)...O(3) _i	1.996(5)		
V(1)...O(2) _{ii}	1.868(1)				
V(2)...O(6)	1.609(6)	V(2)...O(5)	2.157(4)		
V(2)...O(1)	1.792(1)	V(2)...O(3) _{ii}	1.892(2)		
V(2)...O(2) _i	2.346(6)				
V(3)...O(8)	1.596(5)	V(3)...O(5)	1.794(5)		
V(3)...O(6)	2.671(5)	V(3)...O(7) _{ii}	1.887(2)		
V(3)...O(7) _{iii}	2.005(6)				
O(4)-V(1)-O(5)	97.99(25)°	O(4)-V(1)-O(3) _i	103.32(23)		
O(4)-V(1)-O(2) _{ii}	103.97(17)	O(5)-V(1)-O(2) _i	75.90(19)		
O(5)-V(1)-O(2) _{ii}	92.83(17)	O(2) _{ii} -V(1)-O(2) _i	76.61(11)		
O(2) _{ii} -V(1)-O(3) _i	82.03(16)	O(3) _i -V(1)-O(2) _i	82.79(20)		
O(5)-V(2)-O(6)	87.23(24)	O(5)-V(2)-O(2) _i	72.18(19)		
O(5)-V(2)-O(3) _{ii}	84.40(13)	O(6)-V(2)-O(1)	104.51(22)		
O(6)-V(2)-O(3) _{ii}	106.03(21)	O(1)-V(2)-O(3) _{ii}	92.20(6)		
O(1)-V(2)-O(2) _i	96.08(6)	O(2) _i -V(2)-O(3) _{ii}	71.69(15)		
O(8)-V(3)-O(5)	103.27(24)	O(8)-V(3)-O(7) _{iii}	107.28(25)		
O(8)-V(3)-O(7) _{ii}	76.43(18)	O(5)-V(3)-O(7) _{ii}	96.62(16)		
O(5)-V(3)-O(7) _{iii}	149.45(20)	O(7) _{ii} -V(3)-O(7) _{iii}	76.43(18)		

viewed down to the b axis is shown in Fig. 1. The bond lengths and angles around vanadium atoms are given in Table 2. The distance of V-V and Na-O are given in Fig. 1.

References

- 1) J. H. Perlstein and M. J. Sienko, *J. Phys. Chem.*, **48**, 174 (1968).
- 2) J. B. Goodenough, *J. Solid State Chem.*, **1**, 349 (1970).
- 3) N. F. Mott, "Metal-Insulator Transitions," Taylor & Francis, London (1974).
- 4) R. H. Wallis, N. Sol, and A. Zylbersztein, *Solid State Commun.*, **23**, 539 (1977).
- 5) G. Sperlich, W. D. Lazé, and G. Bang, *Solid State Commun.*, **16**, 489 (1975).
- 6) D. Kaplan and A. Zylbersztein, *J. de Phys.*, **37**, L123 (1976).
- 7) W. J. Gunning, A. J. Heeger, R. H. Wallis, N. Sol, and A. Zylbersztein, *Solid State Commun.*, **26**, 155 (1978).
- 8) A. D. Wadsley, *Acta Crystallogr.*, **8**, 695 (1955).
- 9) R. P. Ozerov, G. A. Gol'der, and G. S. Zhdanov, *Soviet Phys. Cryst.*, **2**, 211 (1957).
- 10) The space group A2/m is adopted in Wadsley's paper (Ref. 8).
- 11) S. Etemad, *Phys. Rev. B*, **13**, 2254 (1976).
- 12) R. B. Somoano, A. Gupta, V. Hadek, M. Novotny, M. Jones, T. Datta, R. Deck, and A. M. Hermann, *Phys. Rev. B*, **15**, 595 (1977).
- 13) K. Franulović and D. Djurek, *Phys. Lett. A*, **51**, 91 (1975).
- 14) R. A. Craven, M. B. Salamon, G. DePasquali, R. M. Hermann, G. Stuky, and A. Schultz, *Phys. Rev. Lett.*, **32**, 769 (1974); D. Djurek, K. Franulović, M. Prester, S. Tomić, L. Giral, and J. M. Fable, *Phys. Rev. Lett.*, **38**, 715 (1977).
- 15) R. Comés, "One-Dimensional Conductors," ed by H. J. Keller, Plenum Press, New York and London (1977).
- 16) D. B. McWhan, P. D. Dernier, C. Vettier, A. S. Cooper, and J. P. Remeika, *Phys. Rev. B*, **17**, 4043 (1978); H. Terauchi, *Phys. Rev. B*, **17**, 2446 (1978).
- 17) M. J. Sienko and J. B. Sohn, *J. Chem. Phys.*, **44**, 1369 (1966).
- 18) J. S. Miller and A. J. Epstein, *Progr. Inorg. Chem.*, **20**, 1 (1976).
- 19) A. Friederich, D. Kaplan, and N. Sol, *Solid State Commun.*, **25**, 633 (1978).
- 20) J. J. André, A. Bieber, and F. Gautier, *Ann. Phys.*, **1**, 145 (1976).
- 21) A. Bloch, R. B. Weisman, and C. M. Varma, *Phys. Rev. Lett.*, **28**, 753 (1972).
- 22) R. A. Craven, Y. Tomkiewicz, E. M. Englar, and A. R. Taranko, *Solid State Commun.*, **23**, 429 (1977); S. Etemad, E. M. Englar, T. D. Schultz, T. Penny, and B. A. Scott, *Phys. Rev. B*, **17**, 513 (1978).
- 23) V. K. Kapustkin, V. L. Volkov, and A. A. Fotiev, *J. Solid State Chem.*, **19**, 359 (1976).